[11]R. G. Wheeler and R. W. Ralston, Phys. Rev. Lett. 27, 925 (1971).
[12]Samples were kindly supplied to us by the Semiconductor Research Division of the Forschungslaboratorien Siemens AG, München, Germany.
[13]J. C. Hensel, H. Hasegawa, and M. Nakayama, Phys. Rev. 138, A225 (1965).
[14]W. Kohn, Phys. Rev. 123, 1242 (1961).

Far-Infrared Cyclotron Resonance in the Inversion Layer of Silicon

S. James Allen, Jr., D. C. Tsui, and J. V. Dalton
Bell Laboratories, Murray Hill, New Jersey 07974
(Received 20 November 1973)

Cyclotron resonance in the n-type inversion layer of silicon has been observed at 4.2°K for electron densities between (0.38 and 9.0) $\times 10^{12}/\mathrm{cm}^2$. The electron mass is $m^* = (0.20 \pm 0.01) m_0$ and independent of electron density. The far-infrared mobility decreases monotonically as the electron density increases, in marked contrast to the dc mobility which exhibits a strong maximum in the same range of electron concentrations.

In the surface space-charge layer of a semiconductor, quantization of the electronic motion normal to the surface gives rise to a series of sub-bands, each of which is a two-dimensional continuum of energy levels. Such electronic surface states have been observed in the inversion as well as accumulation layers of a large number of semiconductors.[1] In particular the Si inversion layer has been shown to be an interesting model system for studying the interface properties as well as the scattering processes in a two-dimensional electron gas. We note the recent work of Smith and Stiles[2] and Lakhani and Stiles,[3] who extract from Shubnikov–de Haas (SdH) oscillations an electron mass and a g factor which increase at low electron density. This increase has been attributed to electron-electron renormalization of the mass and g factor.[4,5]

In this paper we report the first observation of electron-cyclotron resonance in the n-type inversion layer of a (100) oriented silicon surface, at 4.2°K, with electron densities in the inversion layer from $(0.38 \text{ to } 9)\times 10^{12}/\mathrm{cm}^2$. The results are most interesting when compared with the transport parameters obtained from dc measurements on the same surface. The resonance experiments show that the cyclotron mass is essentially independent of electron density, in contrast to the SdH mass which increases at low densities. Further, unlike the dc drift mobility at 4.2°K, that falls rapidly at low electron densities,[6] the far-infrared mobility, obtained from the resonance experiment, continues to rise at the lowest electron densities at which it has been measured.

The experiments were performed on the linear metal-oxide-semiconductor field-effect transistor (MOSFET), Fig. 1, which is fabricated on the (100) surface of 10 000 Ω cm p-type silicon wafers, 0.3 mm thick. The oxide was thermally grown to a thickness of 4100 Å. The gate area was $2.5\times 2.5\ \mathrm{mm}^2$. In order to pass the far-infrared radiation, the thickness of the gate electrode was reduced, leaving ≈100 Å of Ti metal with a dc surface resistance of 210 Ω/sq.

The cyclotron resonance between the laser radiation and the inversion layer electrons is detected by measuring the change in the reflectivity of the MOSFET when electrons are introduced into the surface channel. The reflectivity is measured with a homodyne detector formed by a Michelson interferometer shown in Fig. 1. If the inversion layer admittance Y_c is small compared with the substrate admittance, the change in detected power produced by introducing electrons into the inversion layer will be given by the sum of two terms,

$$\Delta P \propto A[\mathrm{Re}(Y_c)\cos\varphi + \mathrm{Im}(Y_c)\sin\varphi] + B[\mathrm{Re}(Y_c)\cos\varphi' + \mathrm{Im}(Y_c)\sin\varphi']. \tag{1}$$

The first term in (1) is caused by the small change in reflected radiation beating with the radiation returning from the reference mirror, whereas the second term is caused by beating the same signal with the radiation reflected from the MOSFET substrate. The constants A and B are determined by numerous experimental factors such as losses encountered in transmission to the MOSFET, reflectivity of the MOSFET substrate, multiple reflections from the MOSFET caused by weak Fabrey-Perot modes established between the lens and MOSFET surface, and the size of the beam at the MOSFET compared with the gate area. However, A and B need be specified only if we are concerned with absolute signal levels or a precise determination of the free-electron density in the channel from the resonance strength. The phase angle φ can be adjusted by moving the reference mirror in Fig. 1. The angle φ' is the relative phase of the small change in reflected radiation produced by channel electrons and that of the radiation reflected by the MOSFET without these electrons. This phase angle φ' is unknown but constant.

Y_c is turned on and off by applying a square-wave gate voltage at 33 Hz and the corresponding changes in power are detected with a lock-in amplifier as the magnetic field, normal to the sample surface, is swept from 0 to 100 kG. At each gate voltage a sequence of four runs has been made corresponding to four different settings of the phase angle φ: $\varphi = \varphi_0 + n\beta/2$, where $n = 0, 1, 2, 3$, and

$$\varphi_0 = \tan^{-1}[\mathrm{Im}(Y_c)/\mathrm{Re}(Y_c)]_{H=0}. \quad (2)$$

Since we do not know φ', we remove that part of $\delta P(H)$ due to the second term in (1) by analyzing only

$$\delta P_1(H) = \delta P(\varphi_0, H) - \delta P(\varphi_0 + \pi, H) \quad (3)$$

and

$$\delta P_2(H) = \delta P(\varphi_0 + \pi/2, H) - \delta P(\varphi_0 + 3\pi/2, H). \quad (4)$$

The radiation incident on the sample is linearly polarized so that the channel admittance may be described by

$$Y_c = \frac{n_s e^2 \omega\tau}{2m^*\omega}\left[\frac{1}{1 + i(\omega - \omega_c)\tau} + \frac{1}{1 + i(\omega + \omega_c)\tau}\right], \quad (5)$$

where n_s is the surface electron density, m^* the effective mass, ω_c the cyclotron frequency, ω the laser frequency, and $1/\tau$ the electron scattering rate. The condition (2) is seen to be

$$\varphi_0 = \tan^{-1}(\omega\tau)$$

and (3) and (4) are given by

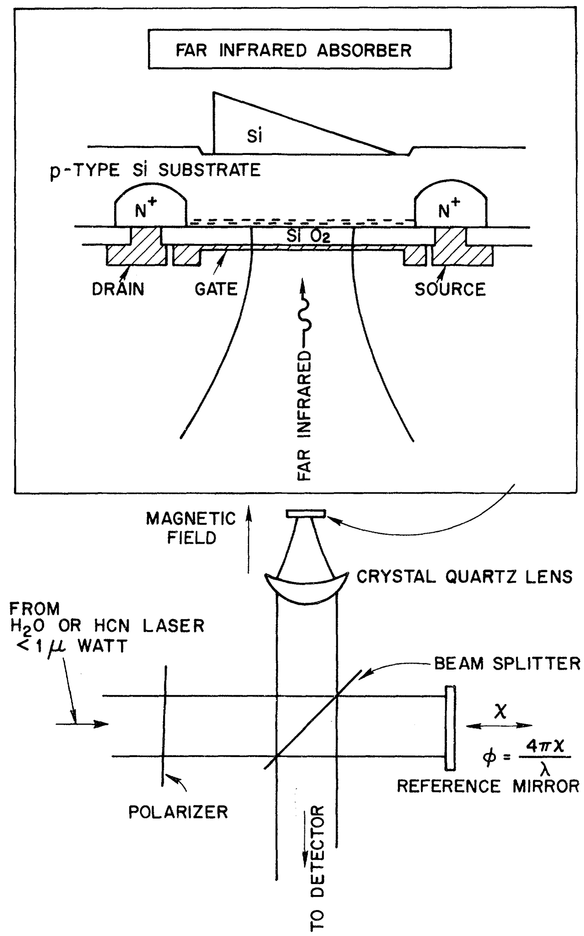

FIG. 1. Michelson interferometer used to measure the MOSFET reflectivity modulated by the inversion layer electrons. Top of figure shows the enlarged view of MOSFET detail.

$$\delta P_1(H) \propto \frac{n_s e^2}{2m^*\omega}\frac{\omega\tau}{[1+(\omega\tau)^2]^{1/2}}\left[\frac{1+(1-\omega_c/\omega)(\omega\tau)^2}{1+(1-\omega_c/\omega)^2(\omega\tau)^2} + (\omega_c \to -\omega_c)\right],$$
$$\delta P_2(H) \propto \frac{n_s e^2}{2m^*\omega}\frac{1}{[1+(\omega\tau)^2]^{1/2}}\left[\frac{(\omega\tau)^2\omega_c/\omega}{1+(1-\omega_c/\omega)^2(\omega\tau)^2} + (\omega_c \to -\omega_c)\right]. \quad (6)$$

The experimental results for a gate voltage of 4.3 V, $n_s = 0.38\times10^{12}/\mathrm{cm}^2$, are shown in Fig. 2. Curves A, B, C, and D correspond to $\varphi = \varphi_0$, $\varphi_0 + \pi/2$, $\varphi_0 + \pi$, and $\varphi_0 + 3\pi/2$, respectively. Although about one half of the "dispersive" and "absorptive" parts occurs above the maximum field, sufficient information is contained in the data to allow an unambiguous measure of m^*, $1/\tau$, and n_s by making a least-squares fit with (6). The results of such a fit are shown in Fig. 2 as dashed lines. At high electron density, weak oscillations

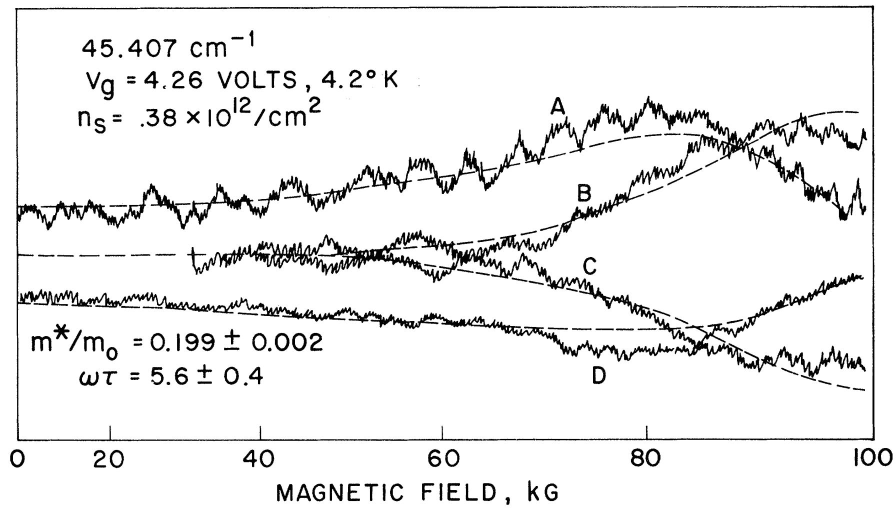

FIG. 2. Detected signal versus magnetic field for the four different settings of the reference mirror described in the text. Dashed curves, least-squares fit to the data with the mass and relaxation time shown. (The horizontal scale is nonlinear in magnetic field. The variation of the noise level from one sweep to the next and the apparent periodic fluctuations, most noticeable in A, are instrumental and have nothing to do with the effects we describe in the text.)

related to the coincidence of the Landau and Fermi levels can be seen, but do not impair the fit. The second term in (1), independent of φ, has first been removed by using (3) and (4) to determine m^*, τ, and n_s and then reintroduced to give a comparison with the actual data. With the exception of a single datum point obtained at 32.12 cm^{-1}, all of the data reported here were obtained at 45.407 cm^{-1} (1360 GHz). The single point at 32.12 cm^{-1} shows that the magnetic field for resonance does indeed scale with frequency in the proper way.

Although the absolute surface electron density n_s cannot be precisely determined from this resonance experiment, because of the uncertainty in A in expression (1), the *relative* n_s at different gate voltages can be determined to ±15%. Within experimental error, n_s obtained from the cyclotron resonance is proportional to the gate voltage measured from the free carrier threshold, as determined from the SdH oscillations. This implies that there is no carrier freezeout down to $n_s = 0.38\times10^{12}/\text{cm}^2$. Further, there is no evidence of occupation of higher sub-bands of different mass up to $9\times10^{12}/\text{cm}^2$.

Figure 3 shows the cyclotron resonance mass determined by these experiments as well as the SdH mass measured by Smith and Stiles.[2] The latter shows an increase at low n_s, which has been ascribed to electron-electron interactions. The cyclotron resonance mass is best described as constant, especially in the range of n_s covered by Smith and Stiles.[2] Its value, $m^* = (0.20\pm0.01)\times m_0$, is slightly greater than the bulk value $m^* = 0.190 m_0$.[7] The difference between the cyclotron resonance mass and the SdH mass at low n_s is beyond the estimated experimental uncertainties. Since *local* cyclotron resonance, in the *absence of electron-lattice interactions*, should measure the "bare" mass, whereas the mass derived from SdH oscillations should be fully dressed,[8] this difference may be attributed to the mass renormalization by the electron-electron interactions.[2]

Figure 3 also shows the electron density dependence of the far infrared mobility together with the dc drift mobility. Both are in qualitative agreement with surface roughness scattering[9] above 2×10^{12}/cm. Below $n_s = 2\times10^{12}/\text{cm}^2$, the mobilities diverge. While the far-infrared mobility continues to increase, the dc mobility drops to zero at the conductance threshold[6] which is ~3.5 V above the free-carrier threshold, of ~1.5 V, determined by extrapolating n_s obtained from the SdH oscillations to zero.[10] We emphasize that in the region where the dc mobility is dropping with gate voltage, n_s determined by the resonance experiment is continuing to scale with the voltage. This fact precludes carrier freezeout as an explanation of the drop in the dc mobility. Furthermore, since the resonance line shape is fitted successfully from 0 to 100 kG, we do not expect a strong dependence of either τ or n_s on

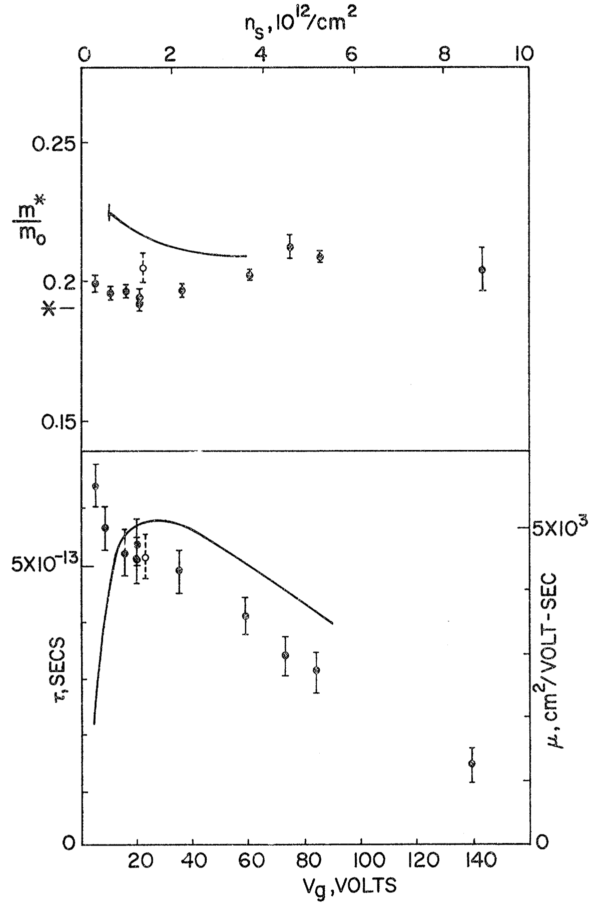

FIG. 3. Top, cyclotron mass versus electron density compared to Ref. 2 (solid line with quoted error); filled circles, 45.407 cm^{-1}; unfilled circles, 32.12 cm^{-1}. Bottom, cyclotron resonance scattering time and mobility as well as the dc mobility measured on the same sample; filled circles, 45.407 cm^{-1}; unfilled circles, 32.12 cm^{-1}; curve, dc results.

the magnetic field. The laser power is sufficiently small to exclude carrier heating by the radiation field.

Stern and Howard[11] have suggested that in the range of low electron densities, where the mobility decreases with decreasing electron density, the scattering may be dominated by interface charges. The far-infrared result can be reconciled with this view only if the characteristic energy associated with this scattering site is less than the laser energy or the energy of the excitations which are created when doing cyclotron resonance. It is also suggested that cyclotron resonance be performed below the conductance threshold where the existence of a real bound state may be detected by a shift in the resonance field. Such experiments are in progress.

It is a pleasure to acknowledge the technical assistance of G. Kaminsky and F. DeRosa. Useful discussions were held with P. J. Stiles and G. A. Baraff.

[1]See, for example, F. Stern, J. Vac. Sci. Technol. 9, 752 (1972), and references contained therein.

[2]J. L. Smith and P. J. Stiles, Phys. Rev. Lett. 29, 102 (1972).

[3]A. A. Lakhani and P. J. Stiles, Phys. Rev. Lett. 31, 25 (1973).

[4]J. F. Janak, Phys. Rev. 178, 1416 (1969).

[5]T. Ando, Y. Matsumato, and Y. Uemura, in *Proceedings of the Eleventh International Conference on the Physics of Semiconductors, Warsaw, 1972,* edited by The Polish Academy of Sciences (PWN—Polish Scientific Publishers, Warsaw, 1972), p. 294.

[6]F. F. Fang and A. B. Fowler, Phys. Rev. 169, 619 (1968).

[7]J. C. Hensel, H. Hasegawa, and M. Nakayama, Phys. Rev. 138, A225 (1965).

[8]W. Kohn, Phys. Rev. 123, 1242 (1961); R. E. Prange and A. Sachs, Phys. Rev. 158, 672 (1967). [See especially Prange and Sachs, Eq. (57).]

[9]R. F. Greene, in *Molecular Processes on Solid Surfaces,* edited by E. Drauglis, R. D. Gretz, and R. I. Jaffee (McGraw-Hill, New York, 1969), p. 239.

[10]The dc mobility is determined from a two-terminal measurement of the conductivity. Although one has some reservation about a two-terminal measurement of the conductivity, four-terminal measurements, fully documented in the literature, show the same maximum in dc drift mobility at $\approx 1.5\times 10^{12}/\mathrm{cm}^2$ as well as the shift of the conductivity threshold from the charge-density threshold. (See, for example, Ref. 6.) The possibility of the channel breaking up into pieces of conducting regions connected by high-resisistance regions may also be discounted. This effect could cause the far-infrared mobility to differ from the dc mobility only if the length scale involved in the breakup were comparable or greater than the far-infrared wavelength, ≈ 100 μm. However, these same dc characteristics are seen in devices with channel widths of only 10 μm.

[11]F. Stern and W. E. Howard, Phys. Rev. 163, 816 (1967).